

X-ray, Micro-Raman, and Infrared Spectroscopy Structural Characterization of Self-Assembled Multilayer Silane Films with Variable Numbers of Stacked Layers

A. Baptiste, A. Gibaud,* and J. F. Bardeau

*Université du Maine, Faculté des Sciences, Avenue O. Messiaen,
UMR 6087 CNRS, 72085 Le Mans Cedex 09, France*

K. Wen, R. Maoz, and J. Sagiv

*Department of Materials and Interfaces, The Weizmann Institute of Science,
76100 Rehovot, Israel*

B. M. Ocko

Brookhaven National Laboratory, Upton, New York 11970

Received September 12, 2001. In Final Form: January 21, 2002

The structure of a series of alcohol-terminated bifunctional long-tail organosilane films with varying numbers of superimposed monolayers (between 1 and 11), prepared on smooth, hydrophilic silicon substrates by the layer-by-layer self-assembly approach, has been investigated with the purpose of elucidating details of the molecular organization and the intra- and interlayer modes of binding in such films. To this end, experimental results obtained by synchrotron X-ray scattering, micro-Raman, and Fourier transform infrared (FTIR) spectroscopic techniques have been combined and compared. A comprehensive analysis of all data demonstrates that the studied multilayer films consist of stacks of uncorrelated discrete monolayers, the inner molecular order of which is preserved with the growing total number of superimposed layers. Similar to self-assembled films of long-tail silanes with terminal $-\text{COOH}$ groups,¹ the intermolecular binding in the present films is characterized by partial intra- and interlayer covalent bond formation. The molecular hydrocarbon tails are perpendicularly oriented on the layer planes, forming a densely packed rotator phase like hexagonal lattice with a molecular surface area of $\sim 20 \text{ \AA}^2$ and a lateral correlation length of the order of 16 molecular diameters.

Introduction

Organized molecular films with predetermined layered structures are currently fabricated by the Langmuir–Blodgett (LB)^{2,3} deposition method and the direct self-assembly of molecules on a solid substrate.^{4–7} Organized molecular films are of particular interest in a variety of applications, for example, in nonlinear optics, tribology, and the development of advanced methods of nanofabrication. As their properties strongly depend on the ability to reproduce the molecular sequence in a faithful manner, determining their structure reliably is of crucial importance. It is well-known, for example, that fatty acid LB films tend to reorganize into polycrystalline phases of the respective bulk materials and so depart significantly from the structure expected on the basis of the deposition protocol. Organized silane films produced by self-assembly offer the great advantage of structural stabilization via multiple covalent and hydrogen bonds, while being more

flexible and less stiff than crystalline LB films of fatty acids. One might thus expect the undisturbed layer structure of silane films to be better preserved, during as well as following the assembly process. It has been further inferred that due to their in-plane molecular mobility, silane films also have the ability of self-healing structural defects of individual layers in a multilayer structure. These extremely robust and versatile materials are therefore remarkable candidates for the design of complex molecular architectures that might have real impact on future nanotechnologies.⁸

In this paper we present a comparative study, using methods of X-ray synchrotron scattering, micro-Raman, and Fourier transform infrared (FTIR) spectroscopies, of a series of self-assembling multilayer silane films prepared by the layer-by-layer technique.¹ The main goal of this study was to define the arrangement of the molecules in the layer planes of the investigated films and provide conclusive experimental evidence demonstrating that planned multilayered architectures of this kind can indeed be prepared with a high degree of perfection and reproducibility in the direction normal to the surface of deposition.

Measurements were carried out on a series of different film samples prepared on smooth silicon wafer substrates (covered with their native oxide layer), going from a single monolayer of OTS (*n*-octadecyltrichlorosilane, $\text{CH}_3(\text{CH}_2)_{17}$ -

(1) Maoz, R.; Sagiv, J.; Degenhardt, D.; Möhwald, H.; Quint, P. *Supramol. Sci.* **1995**, *2*, 9.

(2) (a) Schwartz, D. K. *Surf. Sci. Rep.* **1997**, *27*, 241. (b) Petty, M. C. *Langmuir Blodgett Film: an Introduction*; Cambridge University Press: Cambridge, 1996.

(3) Kuhn, H.; Möbius, D. In *Physical Methods of Chemistry*; Rossiter, B. W., Baetzold, R. C., Eds.; Wiley Press: New York, 1993; p 375.

(4) Maoz, R.; Netzer, L.; Gun, J.; Sagiv, J. *J. Chim. Phys.* **1988**, *85*, 1059.

(5) Keller, S. W.; Kim, H. N.; Mallouk, T. E. *J. Am. Chem. Soc.* **1994**, *116*, 8817.

(6) Ogawa, K.; Mino, N.; Tamura, H.; Hatada, M. *Langmuir* **1990**, *6*, 851.

(7) Thomson, M. E. *Chem. Mater.* **1994**, *6*, 1168.

(8) Maoz, R.; Frydman, E.; Cohen, S. R.; Sagiv, J. *Adv. Matter.* **2000**, *12*, 725.

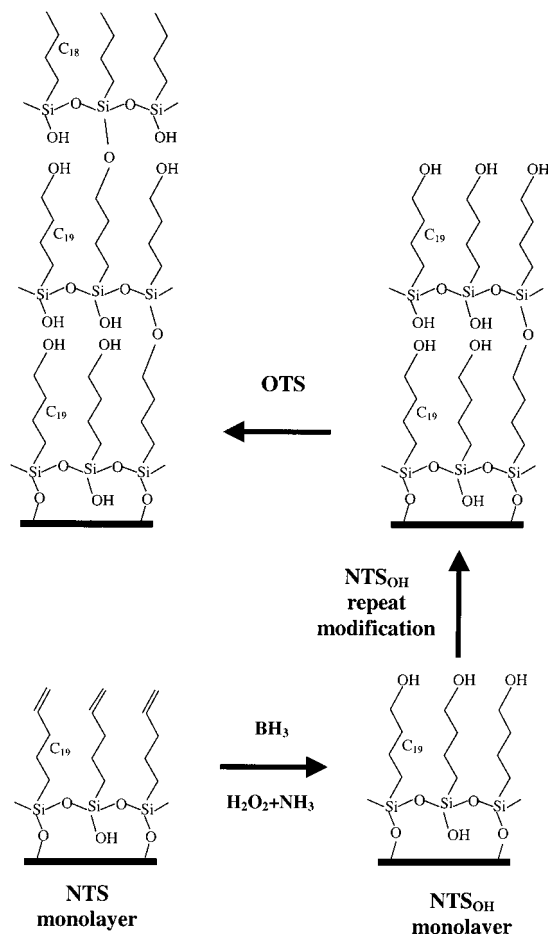


Figure 1. Schematic representation of the layer-by-layer chemical self-assembly of the OTS/(NTSOH)_x/Si films.

SiCl₃) to multilayer OTS/(NTSOH)_x films, where NTSOH is OH-terminated NTS, obtained, as indicated in Figure 1, by the oxidation of the terminal ethylenic function of NTS (18-nonadecyltrichlorosilane, CH₂=CH(CH₂)₁₇SiCl₃), and the number of NTSOH layers, *x*, varies between 1 and 11. Although NTSOH and OTS are similar, both with a silane headgroup and a long hydrocarbon tail, there are significant differences. NTSOH has a terminal CH₂OH alcohol group whereas OTS (18 carbon atoms) is one carbon atom shorter than NTSOH (19 carbon atoms) and is terminated with a CH₃ methyl group.

The layer-by-layer self-assembly process was monitored by quantitative FTIR spectroscopy. X-ray scattering measurements were carried out to probe both the in-plane structure and the layer arrangement in the direction normal to the surface. A quantitative determination of the electron density profile (normal to the surface) of these multilayers was achieved from a self-consistent analysis of the X-ray specular reflectivity, while grazing angle lateral diffraction (GID) measurements allowed the lateral packing motif and the surface area per molecule to be determined. In addition, micro-Raman spectroscopic analysis (without relying on field or resonance enhancement) was used to diagnose the conformation and lateral order of the molecular paraffinic tails in the film.⁹ In particular, the C–H stretching region was carefully analyzed. Indeed, this region has been widely used as a structural probe to provide useful information about the

ordering and the environment of the hydrocarbon moiety in lipids and related systems.^{9–14}

Experimental Section

Thin multilayer films of OTS/(NTSOH)_x/Si were constructed layer-by-layer using the chemically controlled self-assembly procedure presented schematically in Figure 1.¹⁵ In brief, the procedure consists of the following steps: A base monolayer of NTS (gift sample from Dr. K. Ogawa, Matsushita Electric Ind. Co. Ltd., Osaka) was first assembled on a freshly cleaned double side polished Si wafer substrate (Semiconductor Processing Co., (100) orientation, type P, resistivity > 10 Ω cm, 0.5 mm thick, cut into pieces ~20 × 40 mm), by immersion of the hydrophilic substrate for ~5 min in a 5 × 10⁻³ M silane solution in purified bicyclohexyl (BCH) at the ambient temperature, followed by sonication in clean toluene for ~15 s. The NTS monolayer thus produced emerged completely dry from both the adsorption solution and toluene and was subsequently converted to the corresponding alcohol-terminated monolayer, NTSOH. This was achieved by immersion for 5 min in a 1.0 M solution of BH₃ in tetrahydrofuran (BH₃·THF complex, Aldrich) at ambient temperature (after which the surface was thoroughly rinsed with pure water), followed by immersion, for 10 min, in a solution of NH₄OH:H₂O₂:H₂O (1:1:5) at 55 °C, copious rinse with pure water, and final blow off of the wet surface with clean N₂, just before the assembly of the next layer. To build a multilayer, the procedure described above was sequentially repeated, by the self-assembly of a new NTS monolayer on top of an underlying NTSOH one and its subsequent oxidation to NTSOH. In the final step, the film was capped with a top OTS monolayer, thus creating a chemically inert, nonwetable outer film surface.

Micro-Raman experiments were performed at room temperature on a Jobin-Yvon T64000 Raman spectrometer. Laser light of wavelength 5145 Å was generated by a coherent argon–krypton ion laser operating at a power of 40 mW. The spectra were collected with a microscope ×100 objective, which produces a spot size on the sample surface of about 1–2 μm.

Infrared spectra were measured in the Brewster angle configuration, as described before.¹

X-ray reflectivity and grazing incidence X-ray scattering measurements were performed on beam line X22A at the NSLS (National Synchrotron Light Source) with λ = 1.197 Å. For the reflectivity measurements, the incident beam was set by an entrance slit (50 μm by 0.4 mm) and the detector area was set by a detector slit (1 mm × 1 mm) located about 600 mm from the sample. For the diffraction at grazing angles, the detector slit was replaced with soller slits which provide a resolution of 0.1° (full width at half-maximum, fwhm.). The X-ray measurements were carried out in a sealed cell, under vacuum conditions, to minimize the effects of radiation-induced damage.

Raman Measurements

Figure 2 shows unenhanced Raman spectra in the ν(C–H) region for the series of OTS/(NTSOH)_x (with *x* = 1, 4, 7, 11) films. The strongest bands observed at 2882 and 2847 cm⁻¹ are straightforwardly assigned to the methylene antisymmetric (ν_a(CH₂), d⁻) and symmetric (ν_s(CH₂), d⁺) stretching modes, respectively.⁹ We now discuss the information that can be obtained from the analysis of the peak position, width, and intensity of these two bands. The peak position of these bands is known to be chain-length dependent and to depend on the conformation of the hydrocarbon chains. For extended all-trans chains these bands are reported in the range of 2880–

(10) Zerbi, G.; Magni, R.; Gussoni, M.; Moritz, K. H.; Bigotto, A.; Dirlikov, S. *J. Chem. Phys.* **1981**, *75*, 3175.

(11) Okabayashi, H.; Kitagawa, T. *J. Phys. Chem.* **1978**, *82*, 1830.

(12) Almirante, C.; Minoni, G.; Zerbi, G. *J. Phys. Chem.* **1986**, *90*, 852.

(13) Bardeau, J. F.; Parikh, A. N.; Beers, J. D.; Swanson, B. I. *J. Phys. Chem.* **2000**, *B104*, 627.

(14) Gaber, B. P.; Peticolas W. L. *Biochim. Biophys. Acta* **1977**, *465*, 260.

(15) Wen, K. Ph.D. Thesis, Weizmann Institute, submitted April 1999.

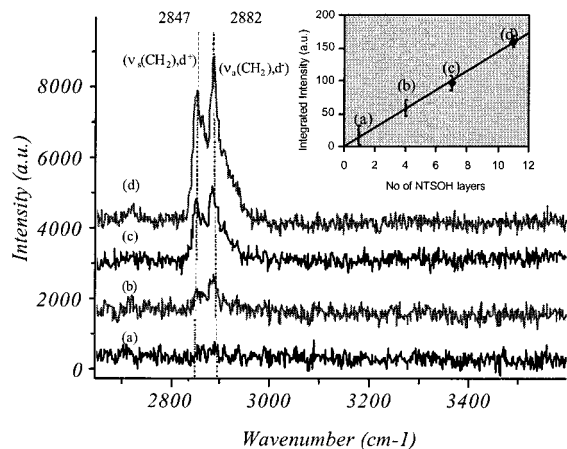


Figure 2. Raman spectra of (a) OTS/(NTSOH)₁/Si, (b) OTS/(NTSOH)₄/Si, (c) OTS/(NTSOH)₇/Si, and (d) OTS/(NTSOH)₁₁/Si in the high-frequency region (2700–3500 cm⁻¹). The inset gives a plot of the integrated intensity of the methylene and methyl C–H stretching modes as a function of the number of NTSOH layers, after subtraction of the intensity of OTS/Si.

2884 and 2845–2850 cm⁻¹, and for liquidlike disordered chains at 2888–2890 and 2850–2853 cm⁻¹.^{16–20} In addition, the narrow bandwidths estimated for the d⁻ and d⁺ modes (fwhm values of 11 and 16 cm⁻¹, respectively) are consistent with those characteristic of the hexagonal (“rotator”) phase of long chain *n*-alkanes (9 and 13 cm⁻¹).⁹ This clearly suggests that the NTSOH molecules assume an essentially all-trans conformation in the multilayer. We should point out that the peak positions of ν_a(CH₂) and ν_s(CH₂) do not vary with the number (*x*) of stacked NTSOH layers, thus confirming their similar molecular orientation and conformation. The Raman intensities of the multilayer were also found to be proportional to the number of stacked NTSOH layers, as shown in the inset of Figure 2. Broad modes around 2900 and 2930 cm⁻¹ were also observed in the present study. They are usually attributed to the Fermi resonance interaction with the continuum of the δ(CH₂) overtone.⁹ The antisymmetric CH₂ mode is forbidden by symmetry from entering into Fermi resonance interaction and is therefore insensitive to environmental changes of the extended chain. On the basis of previous works, the features near 1295 and 1436 cm⁻¹ (and 1463 cm⁻¹) shown in Figure 3 are assigned to CH₂ twisting (T) and scissoring (δ) vibrations of the alkyl chains.^{9,17,20–24} The δ(CH₂) bending mode is dependent on the lateral packing order of the chains. Thus, the identical peak positions in the two curves in Figure 3 further confirm the similar 2D ordering of these multilayers, regardless of total number of stacked layers.

Taken together, the Raman scattering data clearly indicate an essentially all-trans conformation of the hydrocarbon chains in all studied films.

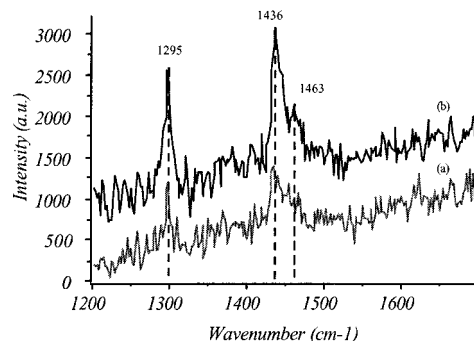


Figure 3. Raman spectra of (a) OTS/(NTSOH)₄/Si and (b) OTS/(NTSOH)₁₁/Si in the C–H deformation vibration region.

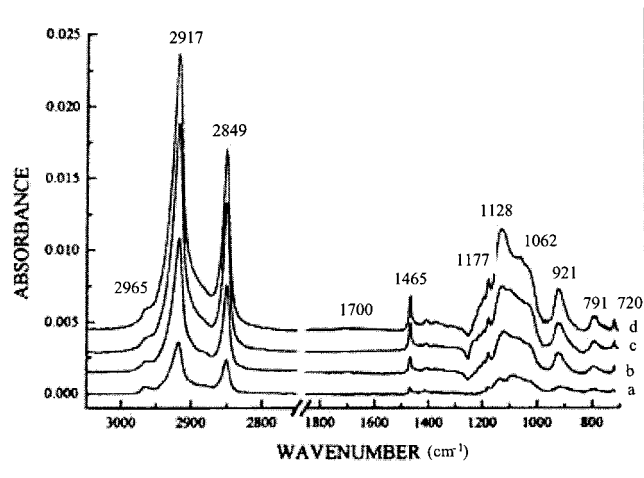


Figure 4. Quantitative Brewster's angle FTIR spectra of (a) OTS/(NTSOH)₁/Si, (b) OTS/(NTSOH)₄/Si, (c) OTS/(NTSOH)₇/Si, and (d) OTS/(NTSOH)₉/Si. The organic films were produced on both sides of the respective double-side-polished silicon wafer substrates.

Infrared Measurements

FTIR spectroscopy was used as a quantitative quality-control tool for routine monitoring of the build-up process of the films. The quantitative conversion of the terminal C=C function of NTS to –CH₂–CH₂OH is indicated by the disappearance of the characteristic C=C bands (around 1643 and 911 cm⁻¹) in the fully reacted NTSOH films and the corresponding proportional growth of the –CH₂– bands with the addition of one CH₂ unit.¹⁵ From the spectra given as examples in Figure 4, one can see that the bandwidths and peak positions of the H–C–H stretch bands, at 2917 and 2949 cm⁻¹, do not change with the number of stacked layers, implying that the organization of the hydrocarbon molecular tails is virtually the same in all films regardless of total film thickness. These data, as well as the progression of sharp methylene deformation bands (coupled CH₂ wag modes) visible between 1177 and 1230 cm⁻¹, are indicative of a “rotator”-phase-like organization of densely packed hydrocarbon chains, oriented perpendicularly on the substrate surface and parallel to one another, in their fully extended all-trans conformation.¹ This is in agreement with the Raman data, and largely confirmed by the analysis of the X-ray data.

The virtually identical surface coverage and molecular organization of each of the discrete monolayers sequentially assembled one on top of the other is further evident from the regular linear growth of all spectral features with the number of deposited layers (Figures 4 and 5). As Figure 5 shows, the sample-to-sample reproducibility is also very good.

(16) Snyder, R. G.; Schachtschneider, J. H. *Spectrochim. Acta* **1963**, *19*, 85.

(17) MacPhail, A.; Strauss, H. L.; Snyder, R. G.; Elliger, C. A. *J. Phys. Chem.* **1984**, *88*, 334.

(18) Amorim da Costa, M.; Geraldies, C. F. G. C.; Teixeira-Dias, J. J. C. *J. Raman Spectrosc.* **1982**, *13*, 56.

(19) Bryant, M. A.; Pemberton, J. E. *J. Am. Chem. Soc.* **1991**, *113*, 8284.

(20) Snyder, R. G.; Strauss, M. L.; Elliger, C. A. *J. Phys. Chem.* **1982**, *86*, 5145.

(21) Chamberlain, J.; Pemberton, J. E. *Langmuir* **1997**, *13*, 3074.

(22) Abbate, S.; Gussoni, M.; Zerbi, G. *J. Chem. Phys.* **1979**, *70*, 3577.

(23) Tashiro, K.; Sasaki, S.; Kobayashi, M. *Macromolecules* **1996**, *29*, 7460.

(24) Beattie, D. A.; Haydock, S.; Bain, C. D. *Vib. Spectrosc.* **2000**, *24*, 109.

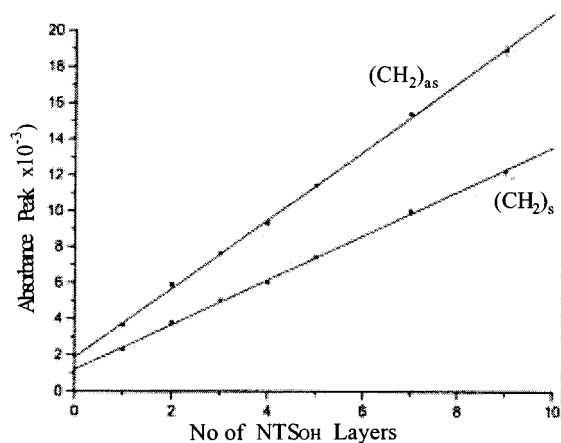


Figure 5. Plot of the peak intensities of the asymmetric and symmetric H–C–H stretch bands (around 2917 and 2849 cm^{-1} , respectively) in the Brewster's angle FTIR spectra of a series of OTS/(NTS_{OH})_x/Si films (as in Figure 1) with variable number (x) of stacked NTS_{OH} layers. As can be seen in Figure 4, the peak positions and bandwidths do not change with the number of stacked layers. It should also be noted that each point in the plot represents a different film sample, produced on a different silicon substrate, the experimental deviation for cases where at least two identically prepared samples were measured being indicated by the point size (for $x=1, 2, 7$) or error bars (for $x=9$).

Finally, the presence of both siloxane (Si–O–Si) stretching modes, around 1100 cm^{-1} , and a Si–OH stretch band, at 921 cm^{-1} (Figure 4), points to the incomplete intra- and interlayer covalent bonding of the silane headgroups.¹ This is confirmed by the analysis of the X-ray data, which allows derivation of a more quantitative evaluation of the intra- and interlayer modes of bonding in these films.

X-ray Grazing Incidence Measurements

Grazing incident angle diffraction (GID) measurements were carried out to determine the in-plane film structure. The intensity distribution as a function of the grazing angle, α , exhibited the characteristic Vineyard peak at the critical angle, α_c , when the in-plane q -vector was set to a scattering peak. Subsequently, α was set to α_c and the scattered intensity distribution was measured as a function of the scattering angle, 2θ , where the in-plane q -vector, $q_{\parallel} = 4\pi/\lambda \sin(\theta)$. The scattering intensity (shown in Figure 6 for $x = 4$ and 7) exhibits a single peak at $q_{\parallel} = 1.51 \text{ \AA}^{-1}$ with a width $\Delta q_{\parallel} = 0.07 \text{ \AA}^{-1}$ fwhm, which is an order of magnitude broader than the resolution. The broad peak gives a correlation length of 80 \AA and indicates that the films are not crystalline. This single peak is characteristic of hexagonal packing with a lattice parameter $a = 4.804 \text{ \AA}$,^{1,25} and the absence of higher order peaks indicates that the form factor falls rapidly with q_{\parallel} . This hexagonal packing was expected from previous GID measurements of silane films, both single layer and multilayer, where only a single GID peak was observed. For single OTS films on silicon, Tidswell²⁵ measured $q_{\parallel} = 1.5 \text{ \AA}^{-1}$, whereas for a five-layer OTS film, Maoz et al.¹ measured $q_{\parallel} = 1.48 \text{ \AA}^{-1}$. Similar hexagonal phases have been observed for bulk n -alkanes in their rotator II phase²⁶

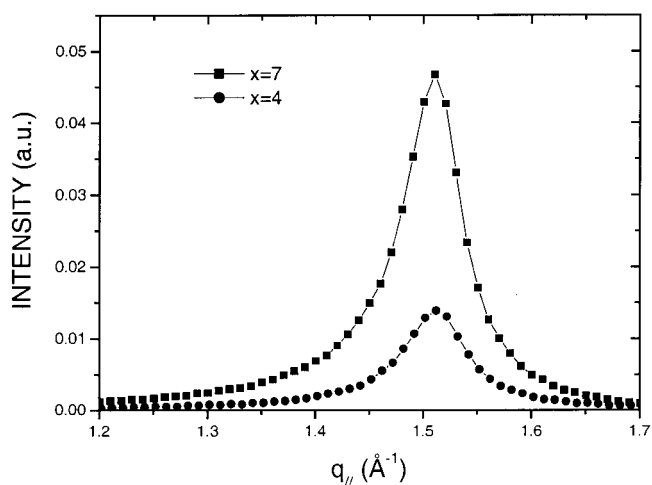


Figure 6. In-plane grazing incident diffraction measurement carried out for $x = 4, 7$ showing a single peak located at $q_{\parallel} = 1.51 \text{ \AA}^{-1}$.

and Langmuir monolayers in their LS phase,²⁷ with q_{\parallel} ranging between 1.51 and 1.53 \AA^{-1} . On the other hand, Langmuir–Blodgett films and Langmuir monolayers typically exhibit an orthorhombic (distorted hexagonal) structure. The calculated area per molecule, $A = 19.98 \text{ \AA}^2$, is identical to that found for the rotator II phase of n -alkanes (20 \AA^2).²⁶

Reflectivity Measurements

In Figure 7 we show the absolute X-ray reflectivity, R , for all films. The reflectivity extends to 0.7 \AA^{-1} , over a dynamic range of 9 orders of magnitude. The relatively high overall intensity and the large modulation intensity indicate that both the film and substrate have angstrom scale roughness. Reflectivity curves of samples with variable x exhibit similarly well-defined Bragg peaks and Kiessig fringes. The Kiessig fringes spacing is inversely proportional to the total film thickness whereas the Bragg peak position is inversely proportional to the layer spacing. Figure 8 shows the refraction-corrected position of the fringes as a function of their number. From a linear fit to the data, it is possible to derive the period of the fringes, which is found to be 0.0442 ± 0.0005 , 0.0313 ± 0.0002 , and $0.01885 \pm 0.00015 \text{ \AA}^{-1}$, for $x = 4, 7$, and 11, respectively. Such a behavior is totally expected, since when x increases, the total thickness should increase linearly with x and, conversely, the Kiessig fringes spacing must inversely decrease. These values respectively yield total film thicknesses $T = 142, 225$, and 333 \AA (with an accuracy of 1 \AA) and, assuming the number of layers is equal to the number of deposition cycles, the length of the repeated NTS_{OH} molecules is so determined. A linear fit to the data yields $T = (27.3 \pm 0.2)x + (33 \pm 1) \text{ \AA}$, x being the number of repeating layers. The average length of one NTS_{OH} molecule is thus $\Lambda = 27.3 \pm 0.2 \text{ \AA}$. This value is consistent with the Bragg peak positions observed for the three samples. The remaining length is the sum of the length of the OTS molecule (i.e., the topmost layer) together with that of the native silicon oxide. It is important to notice that the values thus obtained are model independent.

A quantitative analysis of the reflectivity has been carried out using the matrix method, an exact formulation, rather than the Born approximation which is only valid

(25) Tidswell, I. M.; Rabedeau, T. A.; Pershan, P. S., *J. Chem. Phys.* **1991**, *95*, 42854-2861. Tidswell, M.; Rabedeau, T. A.; Pershan, P. S.; Kosowsky, S. D.; Folkers, J. P.; Whitesides, G. M. *Phys. Rev.* **1990**, *B 41*, 1111.

(26) Sirota, E. B.; King, H. E., Jr.; Singer, D. M.; Shao H. H. *J. Chem. Phys.* **1993**, *98*, 5809.

(27) Kaganer, V. M.; M6hwald, H.; Dutta, P. *Rev. Mod. Phys.* **1999**, *71*, 779. Shih, M. C.; Bohanon, T. M.; Mirkut, J. M.; Zschack, P.; Dutta, P. *J. Chem. Phys.* **1992**, *96*, 1556.

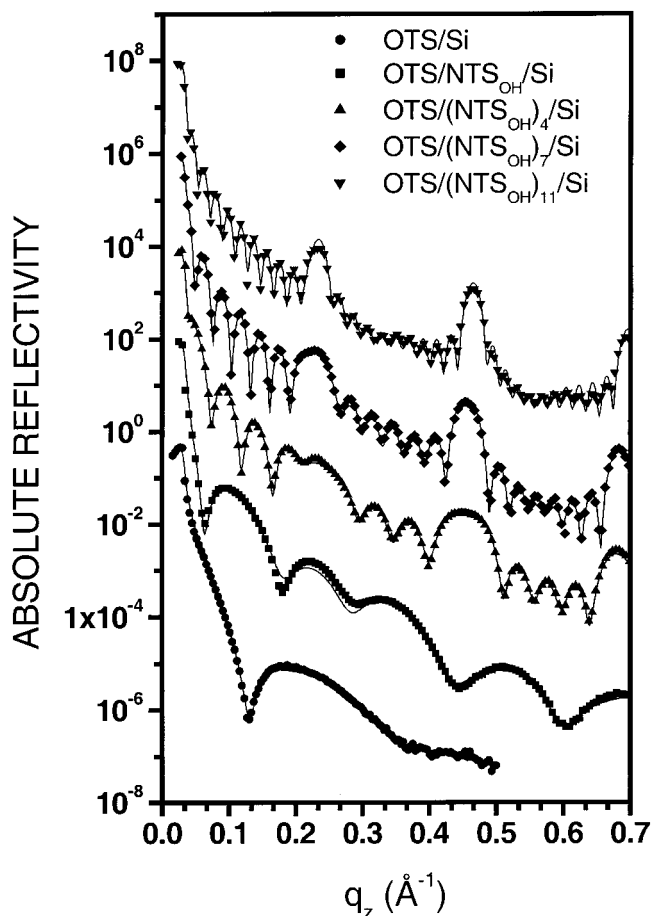


Figure 7. Calculated (full line) and measured (symbols) absolute reflectivity curves for the films with $x = 0, 1, 4, 7,$ and 11 (for clarity, each curve is offset by 10^2 with respect to the previous one).

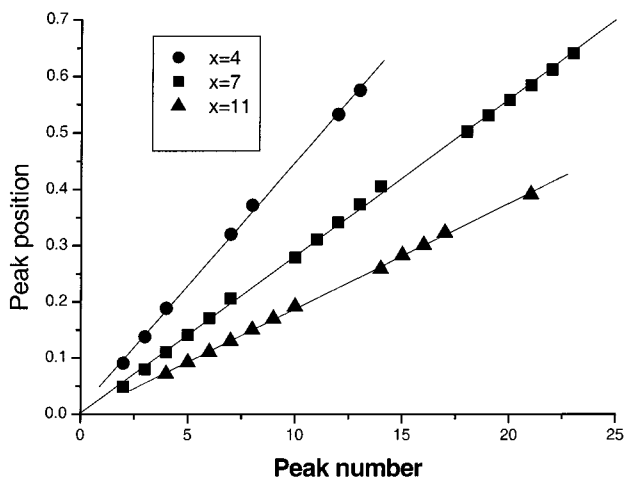


Figure 8. Evolution of the fringe position as a function of its number (for $x = 4, 7,$ and 11), showing a linear behavior.

far from the critical angle.²⁸ The electron density profile is modeled by layers of uniform density ("slabs") which are stacked adjacent to each other. Each slab is parameterized by its electron density and thickness and a smoothing/roughness parameter. In the fitting procedure, these parameters can be either varied or kept fixed.

The most direct representation of the molecular density profile would be to model each of the different molecular

regions, headgroup (silane), middle region (hydrocarbon tail), and the terminal alcohol group (OH), as a slab of constant density with a finite thickness. Thus, each molecular layer would require three different slabs. For simplicity and due to the fact that reflected intensity is weak and difficult to measure above $q_z = 0.8 \text{ \AA}^{-1}$, the number of slabs per layer is reduced to two, by incorporating the contribution of the terminal OH group of each layer in the headgroup of the adjacent silane layer. In addition, the CH_3 terminal group of the topmost OTS layer is taken as part of the CH_2 chain region. Here we have also assumed identical density profiles for each molecular layer in the interior of a multilayer film (translation invariance). The parameters describing the first and last molecular layers are often different since the first layer is bound to the silicon surface and the topmost molecular layer (OTS) is terminated by a methyl group rather than the NTS_{OH} terminal OH group in the interior of the film.

To avoid the refinement of too many correlated parameters, we have performed constrained fits in which most of the parameters were fixed to their expected nominal values. The length of the hydrocarbon chain was fixed at 1.265 \AA per CH_2 unit, which yields a total length of 24.03 and 22.76 \AA for 19C and 18C in the chain, respectively, if, as evidenced by the Raman scattering and FTIR data, the conformation is all-trans. To ensure that the tail of the OTS molecule contains 145 electrons, we fixed the length of the alkyl chain to $22.76 \times 145/144 = 22.92 \text{ \AA}$. The Bragg peak position is then dependent on the length of the headgroup, which was left as a free parameter. In combination with the area per molecule, 19.98 \AA^2 , the density of the alkane region, ρ , is thus fixed at $0.3165e/\text{\AA}^3$. The parameters which are allowed to vary during the fit are therefore the electron density and length of the silane headgroups, the roughness of each interface, and the oxide parameters. It is important to notice that, for X-ray radiation, the index of refraction of silicon oxide is very close to that of silicon, so that including a separate native oxide layer did not improve the fits significantly. However, it was necessary to introduce a thin transition layer ($\approx 4 \text{ \AA}$) between the first NTS_{OH} layer and the substrate itself, with an electron density ($\approx 0.52 \pm 0.03e/\text{\AA}^3$) different from that expected for SiO_2 . This layer can be interpreted as representative of a porous oxide or of the complex interface between the silicon substrate and the organic film itself. One has to keep in mind that the oxide layer and the head of the NTS_{OH} molecule are similar from a chemical point of view so that an exact boundary between the molecule itself and the oxide is difficult to define.

The best reflectivity fits are shown as the solid lines in Figure 7, and they describe all of the essential features of the data, including the fringes and the Bragg peaks. The parameters associated with these fits are listed in Table 1.

The fitting analysis provides a reliable measure of the thickness of the layers, the electron density of the headgroups, and the roughness of the interfaces. As mentioned earlier, the observation of well-defined Kiessig fringes is the signature of atomic-level smooth interfaces. This is confirmed by the fit which yields roughness of the order of $2\text{--}4 \text{ \AA}$. The total thickness of the films is found to be $140.4, 222.7,$ and 329.7 \AA , for $4, 7,$ and $11 \text{ NTS}_{\text{OH}}$ layers, respectively. This is in good agreement with the values obtained directly from the Kiessig fringes positions (Figure 8), however, with a systematic slightly lower total length, by about 1%. If we now consider the length of the repeated NTS_{OH} molecule, for $x = 1, 4,$ and 7 , we find a rather regular value of $27.45 \pm 0.05 \text{ \AA}$, which yields an

(28) Gibaud, A. In *X-ray and Neutron Reflectivity: Principle and Applications*; Dailliant, J., Gibaud, A., Eds.; Springer: Paris, 1999; p 87.

Table 1. The Parameters Used To Fit the X-ray Reflectivity Curves of Films with Growing Number (x) of NTS_{OH} Layers^a

x		oxide	transition layer	repeated NTS _{OH}		top OTS layer	
				head	tail	head	tail
0	ρ (\AA^{-3})	0.697				0.52	0.316*
	thickness (\AA)	25.9				5.15	22.92*
	roughness (\AA)	6.29				2.06	4.1
1	ρ (\AA^{-3})		0.55	0.5	0.316*	0.71	0.316*
	thickness (\AA)		3.4	3.38	24.03*	3.56	22.92*
	roughness (\AA)		4.89	1.94	3.52	2.95	2.1
4	ρ (\AA^{-3})		0.539	0.61	0.316*	0.655	0.316*
	thickness (\AA)		4.6	3.43	24.03*	3.02	22.92*
	roughness (\AA)		3.12	2.77	2.31	2.95	2.4
7	ρ (\AA^{-3})		0.539	0.593	0.316*	0.647	0.316*
	thickness (\AA)		4.55	3.46	24.03*	2.82	22.92*
	roughness (\AA)		2.08	3.03	2.29	3.27	2.1
11	ρ (\AA^{-3})		0.485	0.609	0.316*	0.502	0.316*
	thickness (\AA)		4.86	3.02	24.03*	4.41	22.92*
	roughness (\AA)		2.76	2.19	2.11	3.00	2.0

^a Parameters marked with an asterisk are maintained fixed during the fit.

average length of 3.42 \AA for the headgroup. For $x = 11$, the layer thickness is slightly smaller, with a value of 27.05 \AA .

The total number of electrons in one NTS_{OH} molecule can be obtained from the fitted density parameters along with the measured area, A , and can be expressed as

$$N = A(\rho_{\text{Head}}L_{\text{Head}} + \rho_{\text{Tail}}L_{\text{Tail}})$$

where ρ_{Head} is the electron density of the headgroup and ρ_{Tail} is that of the tail. This yields a total of $N = 186, 194, 193$, and 189 electrons, in the average, in one NTS_{OH} molecule, for increasing values of x . The tail of the molecule (19 CH₂ groups) contains 152 electrons, without the alcohol OH group. If we consider one silicon atom per molecule, the total number of electrons corresponding to oxygen and hydrogen atoms in the head of the molecule becomes $N - 166$. For $x = 1, 4, 7$, and 11, we thus obtain 20, 28, 27, and 23 additional electrons, respectively, in the average, in the headgroup of the NTS_{OH} molecule, which must be assigned to oxygen and hydrogen. For $x = 1$, one may expect this number to be smaller than those corresponding to the higher values of x , since the first NTS_{OH} layer lies on the native oxide of the silicon wafer. Therefore, an alcohol OH group does not contribute to the silane headgroup in this case. The lower value (20 electrons) obtained is thus reasonable.

Information on the interlayer and intralayer cross-linking (polymerization) can be ascertained from the average number of electrons in the headgroup region of the silane molecule. In the absence of cross-linking there are 36 electrons originating from the four OH groups, three of which are attached to the Si atom (silanols) and the remaining one is from the terminal alcohol group of the underlying molecule. For every covalent bond between neighboring molecules, one water molecule is released and 10 electrons are removed from the headgroup region. The average number of water molecules released per NTS_{OH} depends on the average degree of polymerization, n , of a laterally connected siloxane polymer and the fraction, r , of molecular headgroups that have interlayer covalent bonds. Within the layer plane, the average number of electrons per NTS_{OH} molecule is reduced by $10(1 - 1/n)$, and between the planes, the number of electrons is reduced by $10r$. Therefore, in terms of n and r , the average number of O and H electrons per silane molecule in the headgroup region (except for the first

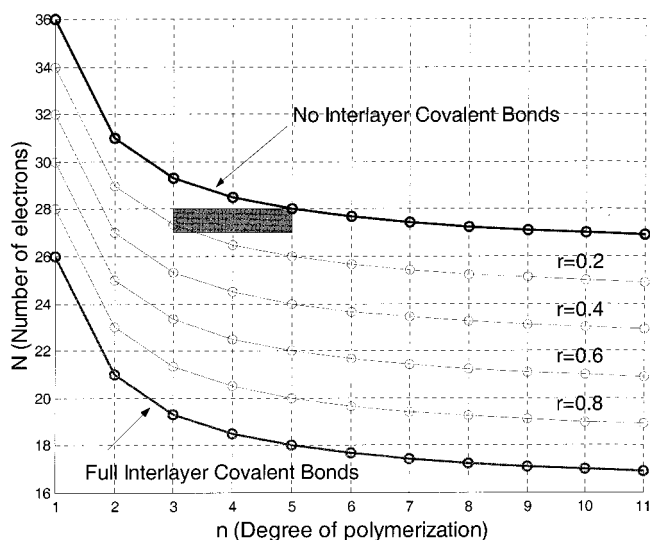


Figure 9. Evolution of the average number of oxygen and hydrogen electrons (N) in the headgroup of one NTS_{OH} molecule (including the contribution of the terminal alcohol OH groups from the underlying layer of NTS_{OH} molecules) as function of the average degree of intralayer (lateral) polymerization (n) and the fraction of molecular headgroups having interlayer covalent bonds (r). The region of interest is highlighted.

NTS_{OH} layer) is given by

$$N = 36 - 10(1 - 1/n) - 10r = 26 + 10(1/n - r)$$

The evolution of the average number of O and H headgroup electrons, N , as a function of the average degree of in-plane lateral polymerization, n , for various interlayer covalent bond fractions, r , is shown in Figure 9. One can clearly observe that the number of electrons located in the headgroup should decrease with both the degree of lateral polymerization and the fraction of interlayer covalent bonds. For example, in a lateral dimer without interlayer covalent bonds, NTS_{OH} would have 31 electrons in the headgroup, including the alcohol OH group contributed by NTS_{OH} from the underlying layer. A situation in which 28 electrons are found in the headgroup might represent a pentamer with no interlayer covalent bonds. Increasing the degree of polymerization has therefore the direct effect of reducing the number of electrons in the headgroup. A similar but stronger effect is obtained by increasing the number of interlayer covalent bonds. For example, fully covalently bonded ($r = 1$) interlayer monomers and lateral dimers would have 26 and 21 electrons per molecule in the headgroup, respectively, which shows that full interlayer covalent bonding would have a severe effect on the reduction of the number of headgroup electrons.

The rather extensive intralayer covalent bonding evident in all films, from the presence of complex siloxane (Si-O-Si) bands around 1100 cm^{-1} in their infrared spectra (Figure 4), rules thus out the possibility of a high percentage of interlayer covalent bonds. Therefore, $N = 28 - 27$ (for $x = 4, 7$) suggests a situation intermediate between an unlikely lateral decamer ($n = 10$) without interlayer covalent bonds and an unrealistic lateral dimer with an average proportion of 30–40% of the headgroups having interlayer covalent bonds. A more likely situation, consistent with the infrared evidence, would be to take $n \approx 3-5$, with less than 20% of the headgroups having interlayer covalent bonds (highlighted region in Figure 9). The lower electron density of the molecular headgroup ($N = 23$) obtained for $x = 11$ would similarly correlate

with $n \approx 8-10$ and ca. 40% of the headgroups having interlayer covalent bonds. While the infrared data suggest a tendency for a somewhat higher degree of polymerization in the thicker films (Figure 4), these figures are, most likely, gross overestimates of the actual situation. This has to do with the rather low sensitivity of N to very large variations in the value of n , for $n > 4$ (Figure 9), which may result in unrealistic n values for deviations in N that lie within the experimental error of the fitting procedure. Here, the lower N value obtained for the 12-layer film ($x = 11$) mainly reflects the smaller thickness of the headgroup slab, by ~ 0.4 Å, derived from the fit of the reflectivity curve (Table 1). One can see that, in this case, the last Bragg peak is slightly shifted toward higher wave vector values (Figure 7), which, in turn, means that the molecules appear slightly shorter. A small tilt of the molecular tail could be responsible for this change; however, to maintain a consistent treatment, we decided to adopt constrained fits in which the tail lengths were kept fixed and identical for all films. Combining the X-ray analysis with XPS (X-ray photoelectron spectroscopy) data, from which direct information on the average number of oxygen atoms per molecule can be obtained, will be shown to permit a more reliable evaluation of the intra- and interlayer covalent bonding in such films.²⁹

In the present analysis of the X-ray data, we have shown that the same constrained model applied to all films in a series of multilayers could reproduce fairly well the entire set of reflectivity data. We believe that this is a good signature for the validity of such a model, leading to characteristic molecular lengths and electron densities in agreement with values previously reported in the literature for similar films of long-tail amphiphiles.^{1,30-32}

Conclusions

In this combined Raman, infrared, and X-ray reflectivity study of a series of layer-by-layer self-assembled films,

(29) Wen, K.; Maoz, R.; Cohen, H.; Sagiv, J.; Gibaud, A.; Desert, A.; Ocko, B. M. To be submitted.

(30) Robinson, I. K.; Tweet, D. J. *Rep. Prog. Phys.* **1992**, *55*, 599.

(31) Als-Nielsen, J.; Jacquemain, D.; Kjaer, K.; Leveiller, F.; Lahav, M.; Leiserowitz, L. *Phys. Rep.* **1994**, *246*, 251.

(32) Maoz, R.; Matlis, S.; DiMasi, E.; Ocko, B. M.; Sagiv, J. *Nature* **1996**, *384*, 150.

we have shown that planned multilayer architectures of long-tail silanes can be produced with almost perfect uniformity in the direction normal to the surface of growth. From the Raman scattering and IR data we find that, whatever the number of stacked layers, x , the alkyl tails are always fully extended in their all-trans conformation. X-ray grazing incidence diffraction measurements gave an area per molecule, $A = 19.98$ Å², quite similar to the one reported for "rotator" phases of related n -alkane molecules. The X-ray reflectivity was analyzed with a simple constrained model which describes fairly well the electron density of such films and gives a reasonable interpretation of their structure, both with respect to the length of the alkyl tails and to the number of electrons in the headgroups of the silane molecules. In particular, we find from the position of the Kiessig fringes that the length of a NTS_{OH} molecule is $\Lambda = 27.3 \pm 0.2$ Å. The fitting procedure of the reflectivity data yields an average value of $\Lambda = 27.35 \pm 0.15$ Å. In addition, the average number of O and H electrons in the silane headgroup, including the contribution of the alcohol OH groups of the underlying NTS_{OH} layer, is found to be of the order of 28 ± 1 , for $x = 4$ and 7. This result allows an estimation of the average degree of interlayer polymerization together with the fraction of interlayer covalent bonds, the two values being inseparable on the basis of the X-ray data only. Taking into account also evidence furnished by the infrared data, we conclude that the present results are consistent with a small average degree of interlayer polymerization, together with a small fraction of interlayer covalent bonds.

Acknowledgment. This research was supported by a grant from the United States–Israel Binational Science Foundation (BSF), Jerusalem, Israel, by the French ACI Nanostructure and by the French–Israeli Scientific and Technical Cooperation Program Arc-En-Ciel-Keshet. We thank Dr. K. Ogawa of Matsushita Electric Ind. Co., Osaka, for supplying the NTS material. Brookhaven National Laboratory is supported by U.S. DOE Contract No. DE-AC02-98CH10886.

LA015572R